

Supporting Information

Chemoproteomic Profiling of Lysine Acetyltransferases Highlights an Expanded Landscape of Catalytic Acetylation

David C. Montgomery, Alexander W. Sorum, and Jordan L. Meier *

Chemical Biology Laboratory, National Cancer Institute, Frederick, MD, 21702

Table of Contents for Supporting Information

	<u>Page</u>
Figure S1: Phylogenetic tree of canonical KAT enzymes	S3
Figure S2: Structures of parent KAT bisubstrate inhibitors 4-6	S4
Figures S3-5: Inhibition of recombinant KAT activity by bisubstrates 1-6	S5
Figures S6: Dependence of KAT labeling on probe, photocrosslinking, Cu ²⁺	S8
Figure S7: Inhibition of pCAF labeling by competitor 5 : dose-response	S9
Figure S8: Probe selectivity for KATs at high probe concentration	S10
Figure S9: Competitive labeling of p300 in presence of C646.	S11
Figure S10: LC-MS verification of Gcn5 propionyl/butyryltransferase activity	S12
Figure S11: Labeling of p300/pCAF spiked into HeLa proteomes	S13
Figure S12: Western blot of Gcn5/CBP levels in HeLa whole cell extracts	S14
Figure S13: Expanded phylogenetic tree of KAT and characterization methods	S15
Figure S14: Model separation of KAT substrate peptides for inhibition analysis	S16
Figure S15: Structure of click reagents 8 and 9	S17
Scheme S1: Synthesis of Lys-CoA-BPyne probe 1	S18
Scheme S2: Synthesis of H3K14-CoA-BPyne probe 2	S19

Table S1: Spectral counts for HEK-293 proteomic enrichments by probe 2	S20
Table S2: Spectral counts for HeLa proteomic enrichments by probe 1	S21
Table S3: Uniprot accession numbers and references for orphan KATs	S22
General synthetic procedures	S23
Synthesis of KAT photoaffinity probes and parent bisubstrates	S24-27
Characterization data for KAT chemoproteomic probes	S28-33
References	S34-34

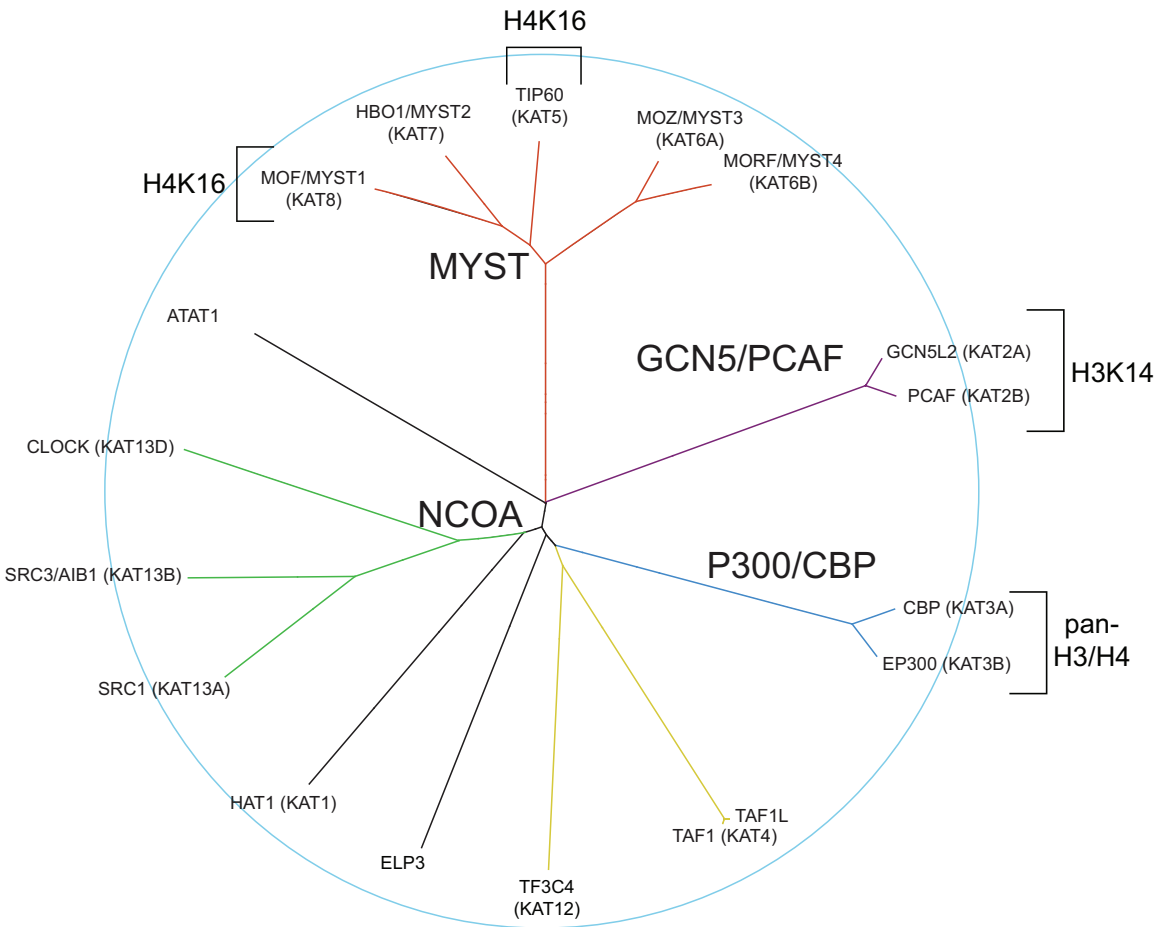


Figure S1. Canonical human lysine acetyltransferases identified by Arrowsmith et al.¹

Alignment file obtained from the Structural Genomics Consortium

(http://apps.thescg.org/resources/phylogenetic_trees/, accessed December 4, 2013).²

Individual KATs are grouped into families with cognate histone substrates.

Key: H3K14Ac = histone H3 lysine 14 acetylation activity. H4K16 = histone H4 lysine 16 acetylation activity. Pan-H3/H4 = multiple histone H3 and H4 acetylation substrate residues characterized.

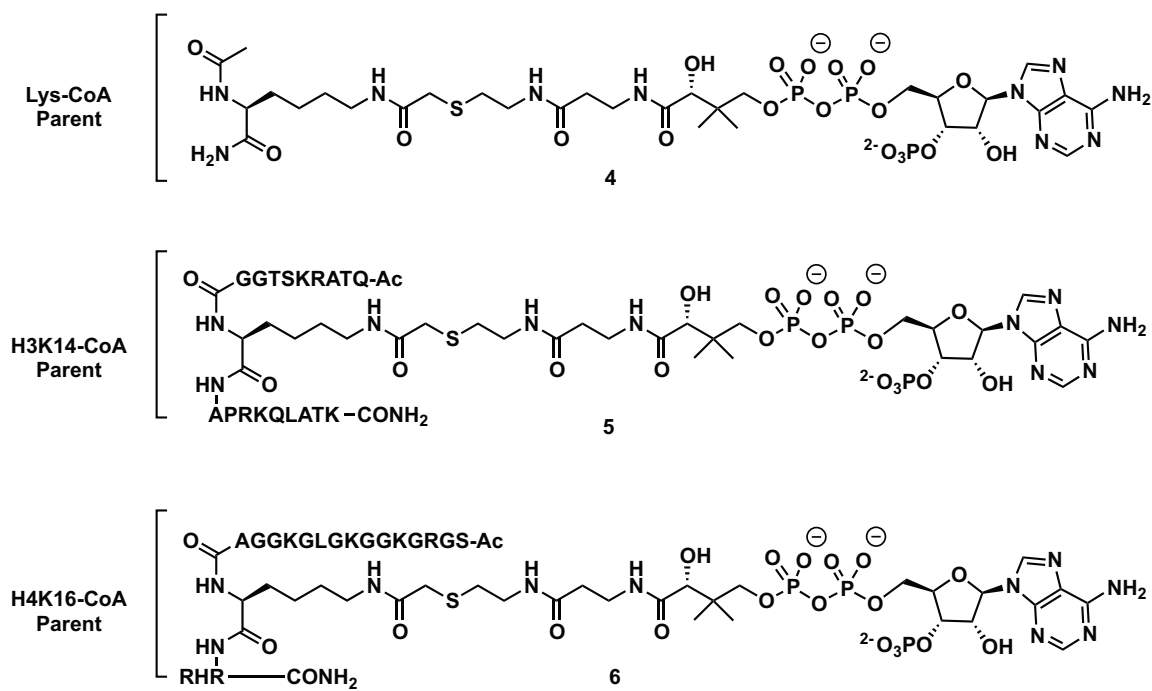


Figure S2. Structures of parent KAT bisubstrate inhibitors **4-6**

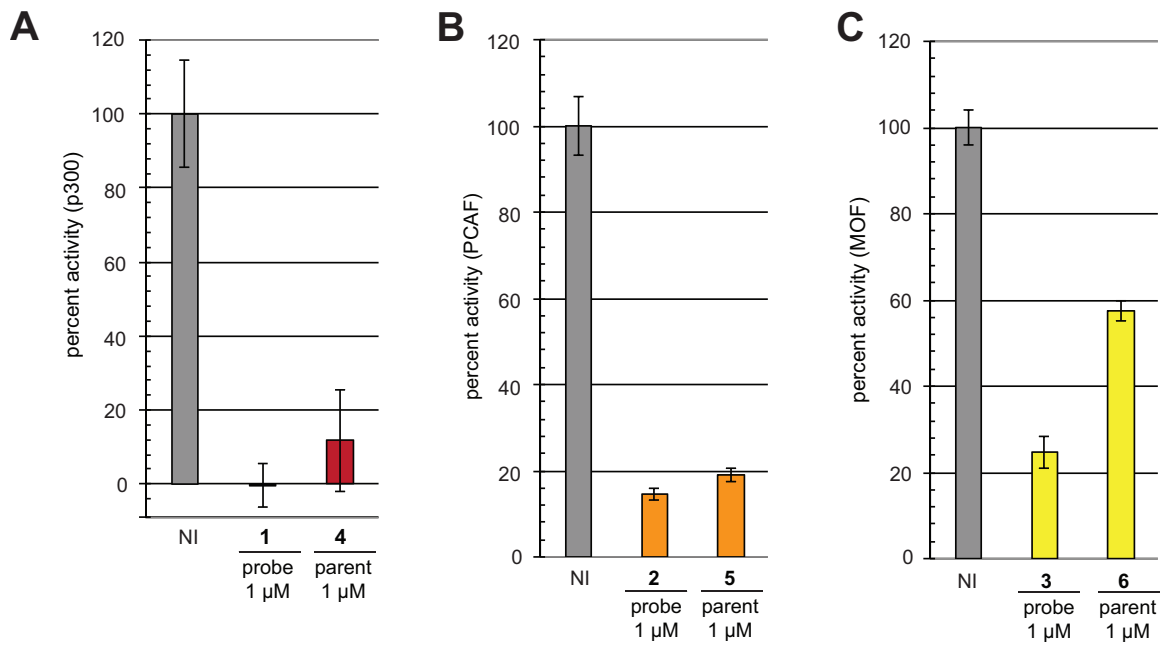


Figure S3. Inhibition of recombinant KAT activity by bisubstrates **1-6**. (a) Inhibition of p300 by KAT bisubstrates **1** (probe) and **4** (parent). (b) Inhibition of pCAF by KAT bisubstrates **2** (probe) and **5** (parent). (c) Inhibition of Mof by KAT bisubstrates **3** (probe) and **6** (parent).

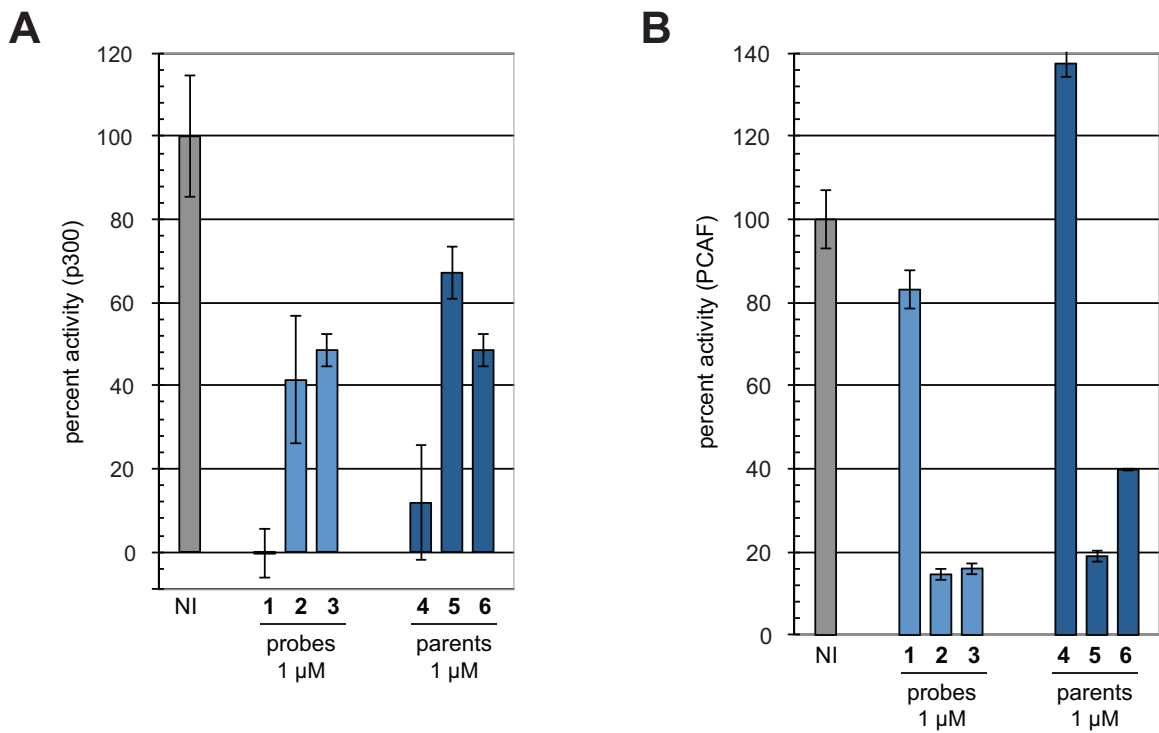


Figure S4. Selectivity of KAT inhibition by chemoproteomic probes. (a) Relative inhibition of p300 by probes **1-6**. Lys-CoA probes (**1, 6**) show the most potent inhibition of p300. (b) Relative inhibition of pCAF by probe **1-6**. H3K14-CoA probes (**2, 5**) show the most potent inhibition of pCAF.

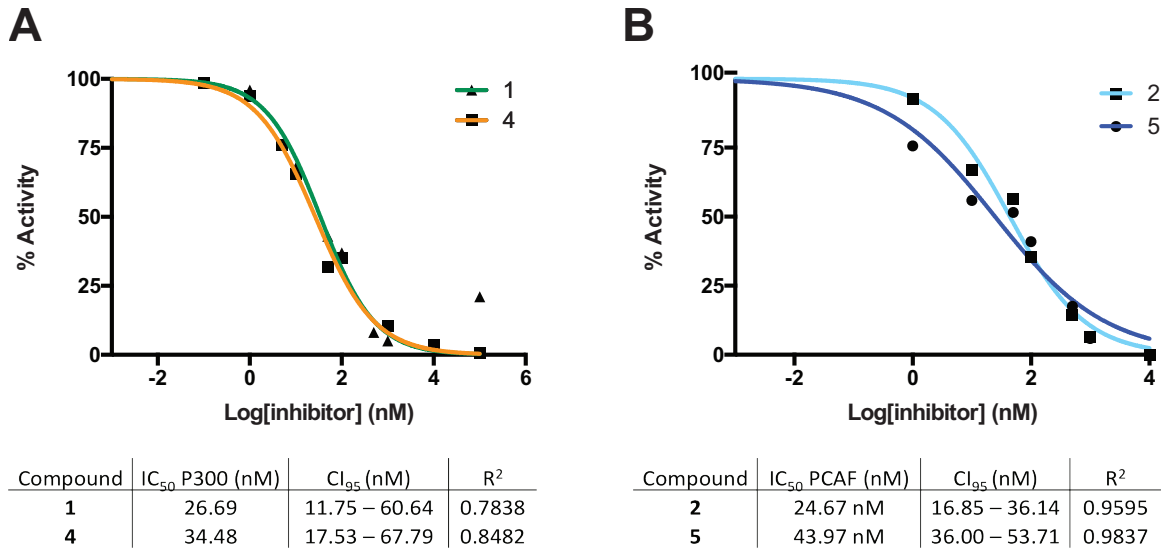


Figure S5. Dose-response analysis of KAT inhibition by chemoproteomic probes and parents. (a) p300. (b) pCAF.

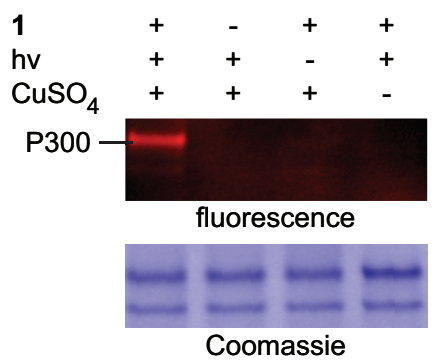
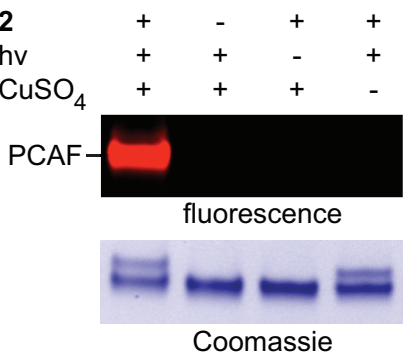
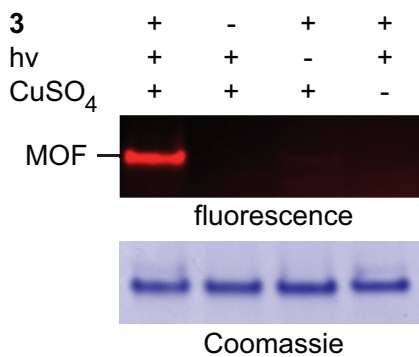
A

Figure S6. Dependence of KAT labeling on probe, photocrosslinking, and Cu²⁺ (a) Lys-CoA-BPyne **1**. (b) H3K14-CoA-BPyne **2**. (c) H4K16-CoA-BPyne **3**.

B**C**

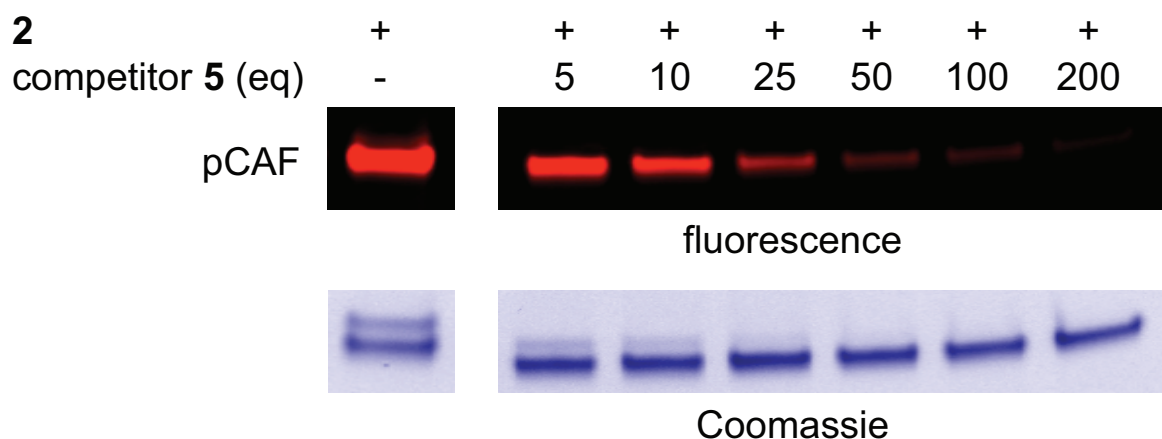
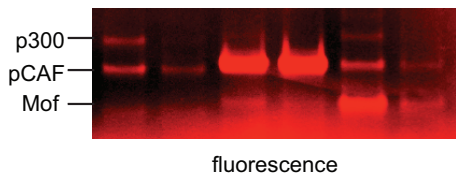


Figure S7: Competitive inhibition of pCAF labeling by parent bisubstrate inhibitor **5**: dose-response.

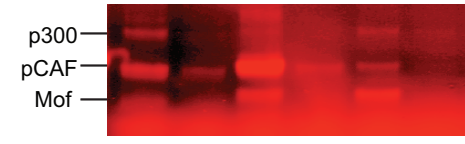
a 1 μM probe

1	+	+	-	-	-	-
2	-	-	+	+	-	-
3	-	-	-	-	+	+
4 (comp)	-	+	-	+	-	+



b 1 μM probe

1	+	+	-	-	-	-
2	-	-	+	+	-	-
3	-	-	-	-	+	+
4 (comp)	-	+	-	-	-	-
5 (comp)	-	-	-	+	-	-
6 (comp)	-	-	-	-	-	+



10 μM probe

1	+	+	-	-	-	-	
2	-	-	+	+	-	-	
3	-	-	-	-	-	+	+
4 (comp)	-	+	-	-	-	-	-
5 (comp)	-	-	-	+	-	-	-
6 (comp)	-	-	-	-	-	-	+

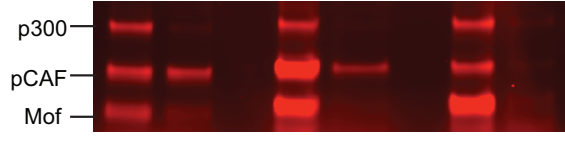


Figure S8: Additional data for in vitro labeling of KAT enzymes by probe **1-3**. (a) Competition of probe labeling (1 μM) by Lys-CoA (100 μM). Probes **1** and **3** are specifically competed, while probe **2** efficiently labels pCAF in the presence of Lys-CoA. (b) Comparison of probe labeling at low (1 μM) and high (10 μM) concentrations. Probes **1-3** label KATs from each family at high concentrations.

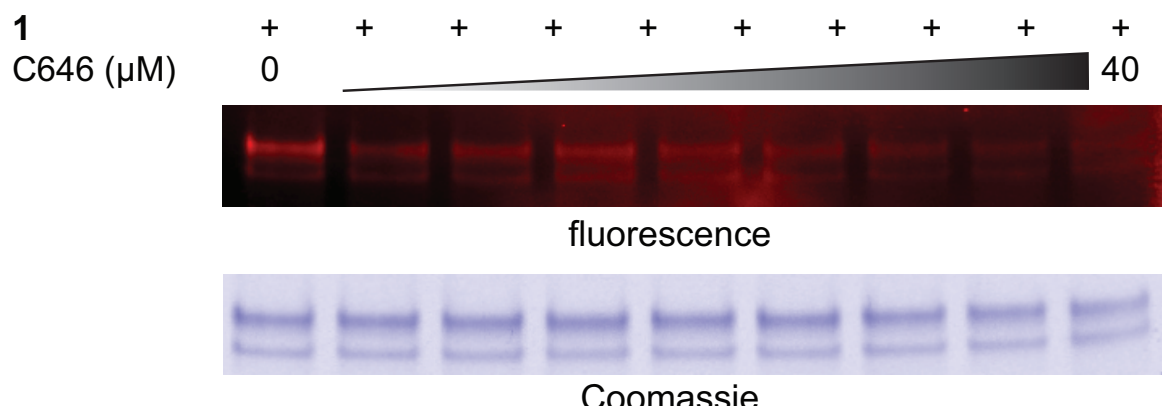


Figure S9. Competitive labeling of p300 in presence of C646.

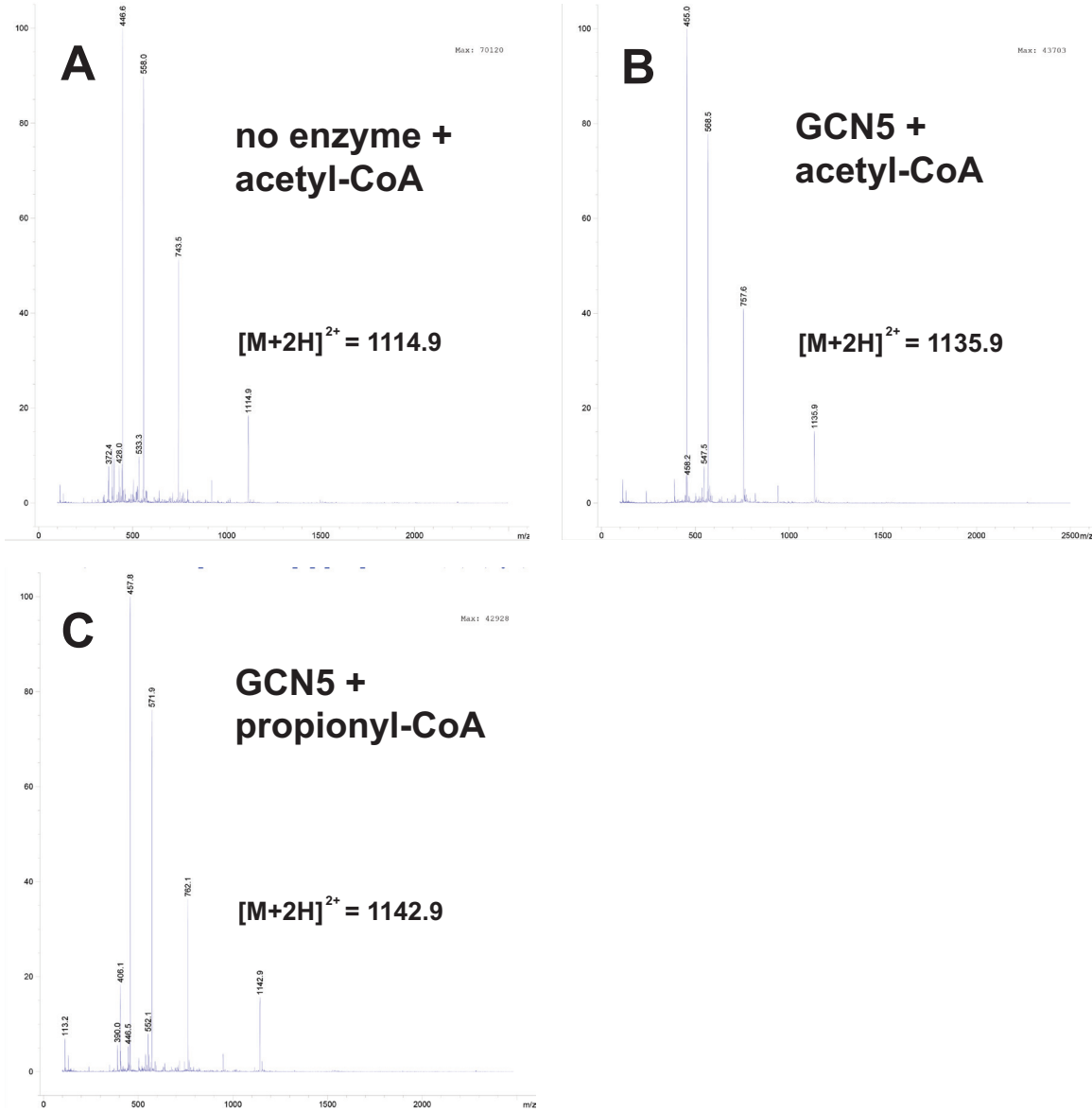


Figure S10. LC-MS/MS analysis of Gcn5 acyltransferase activity. (a) Native peptide (no enzyme) (b) GCN5 + peptide + acetyl-CoA (c) GCN5 + peptide + propionyl-CoA.

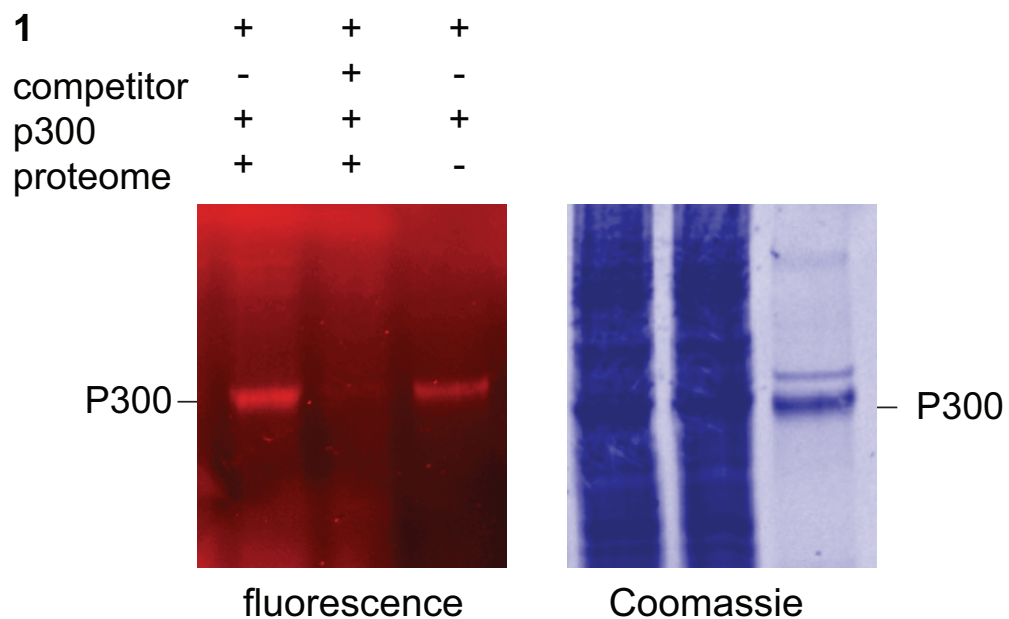
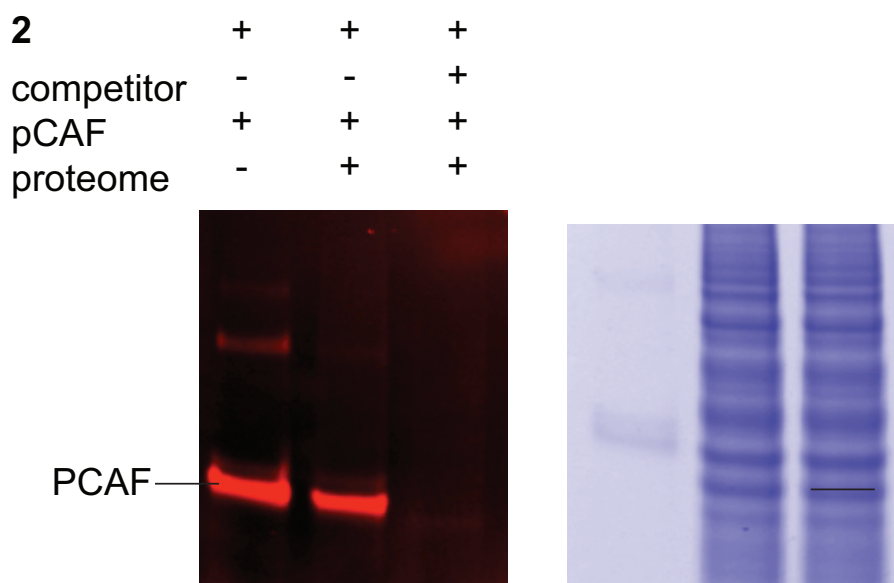
A**B**

Figure S11. Labeling of p300 and pCAF spike-ins in HeLa cell extracts. Enzyme amounts: p300 (17 pmols), pCAF (7 pmols).

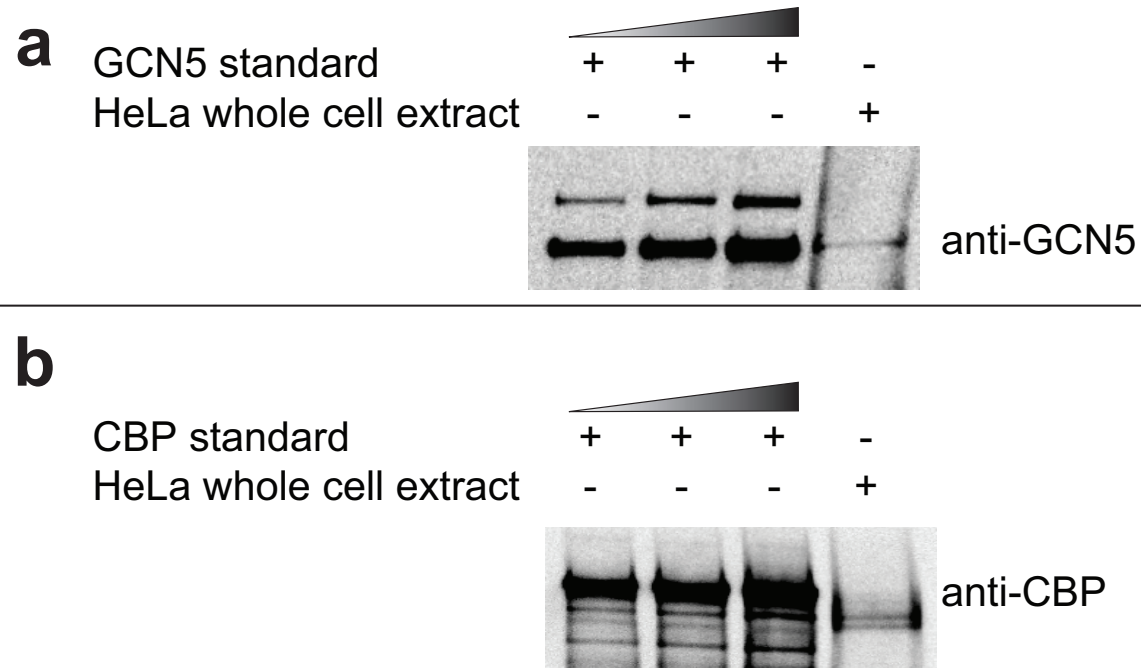


Figure S12. Expression of CBP in HeLa whole cell extracts. HeLa whole cell extracts (25 ug) were blotted for using anti-CBP antibodies (Cell Signaling Technologies). For comparison, commercial HeLa cell nuclear extracts were analyzed in dose response (15, 20, 25 ug). Attempts to label/enrich commercial HeLa cell nuclear extracts were unsuccessful due to protein denaturation, as judged by FP-labeling and KAT activity assays.

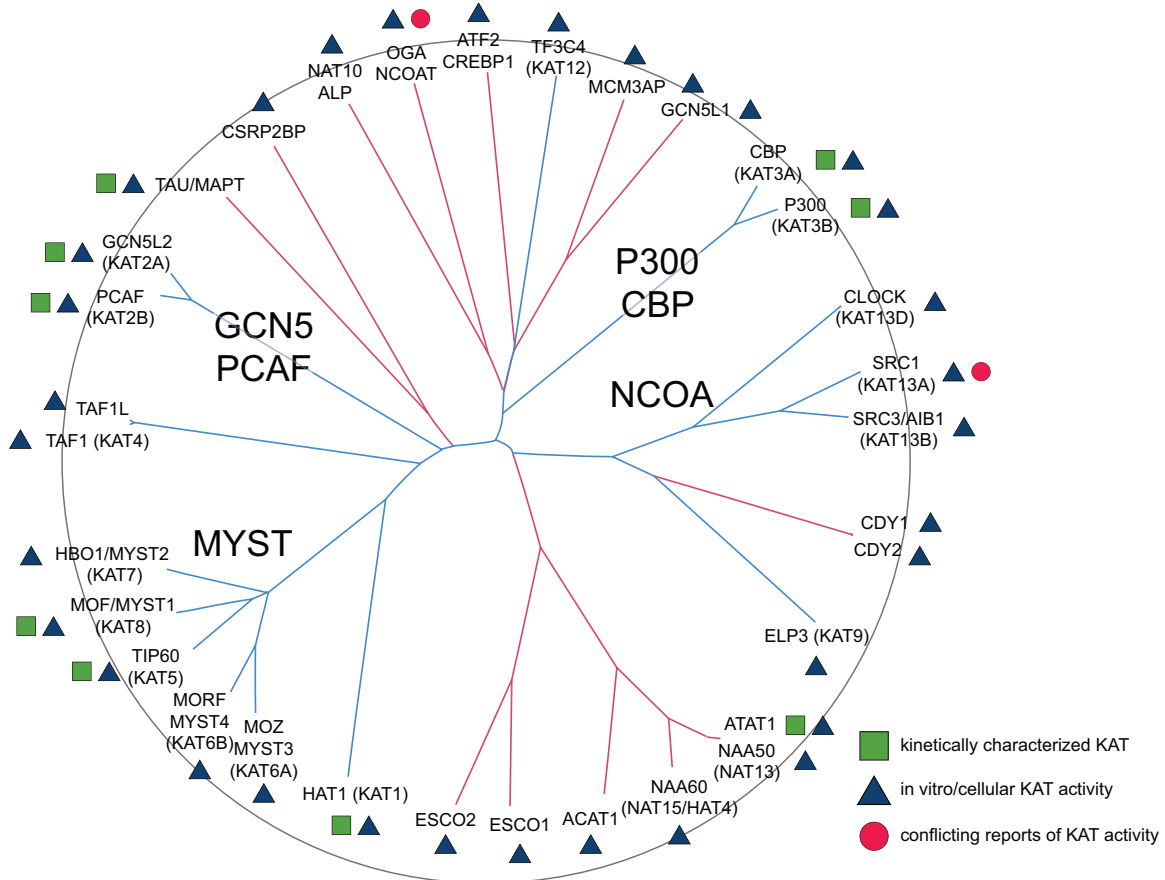


Figure S13. Phylogenetic tree of KATs with coded summary of evidence for KAT activity. Uniprot accession numbers and references for all KATs are provided in Table S1.

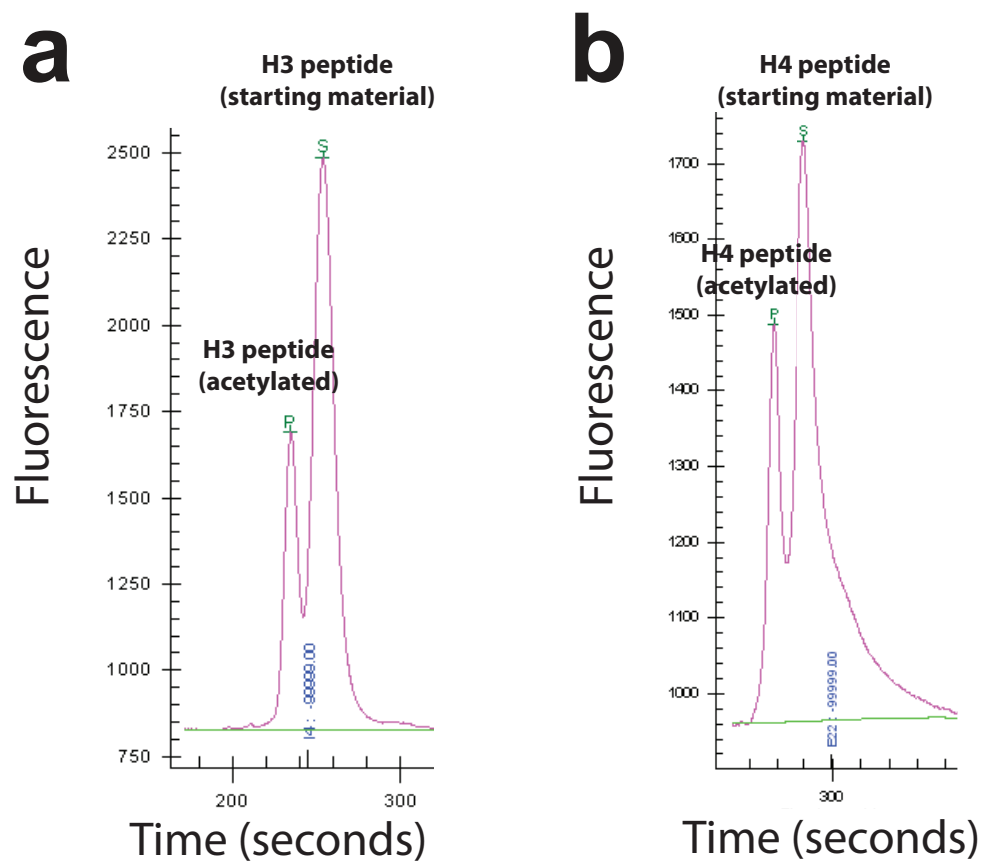
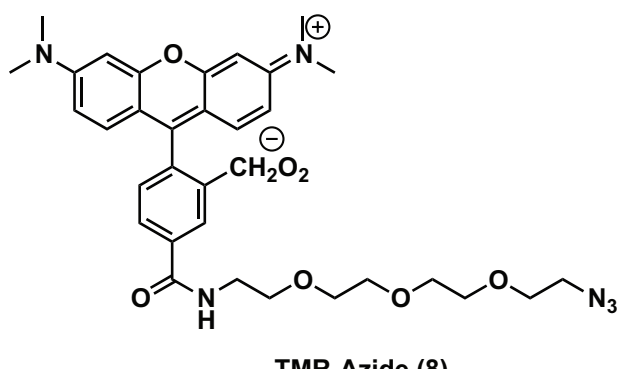
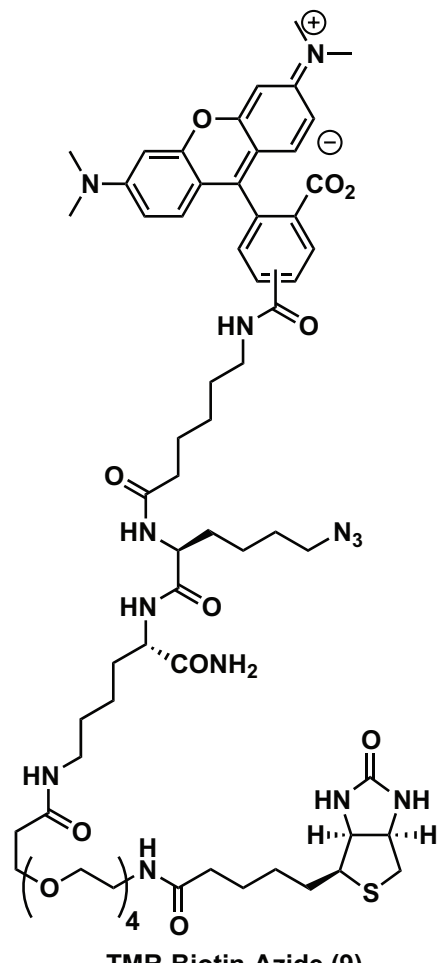


Figure S14. Schematic of separation-based assay for KAT activity. (a) H3(5-23)-FITC peptide (1 μ M) incubated in presence of pCAF (10 nM), acetyl-CoA (5 μ M). (b) H4(1-19)-FITC peptide (1 μ M) incubated in presence of p300 (50 nM) and acetyl-CoA (5 μ M). Peptide substrate and product identities were confirmed by LC-MS analysis.

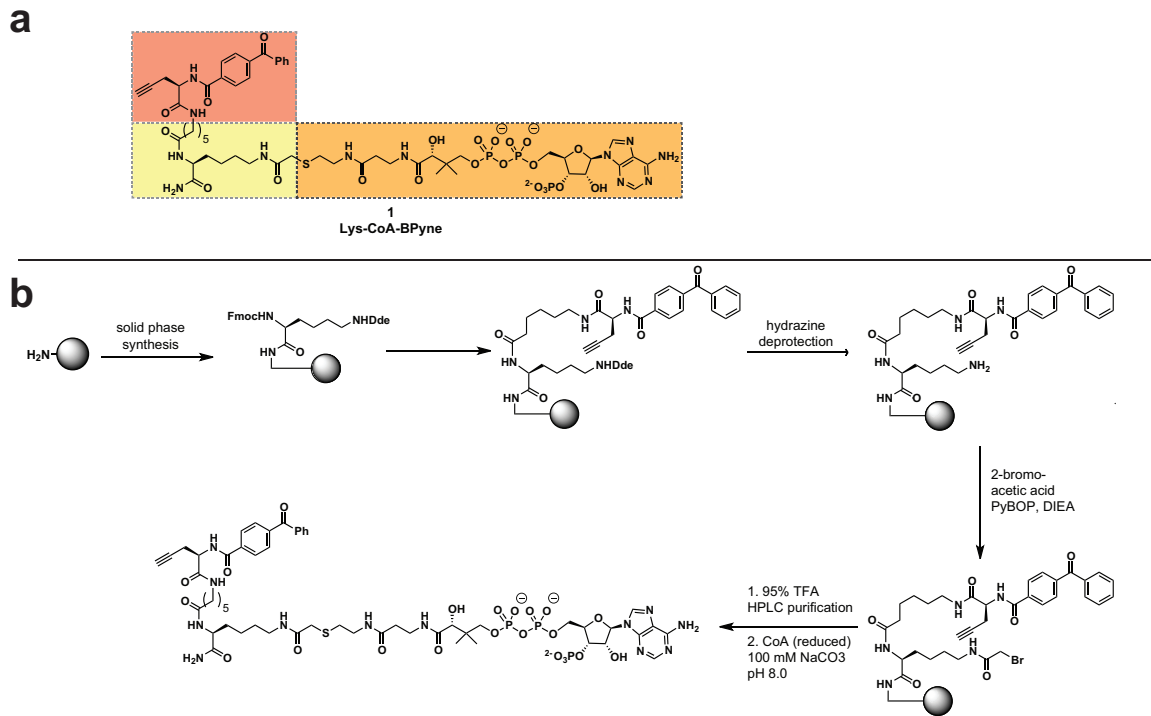


TMR-Azide (8)

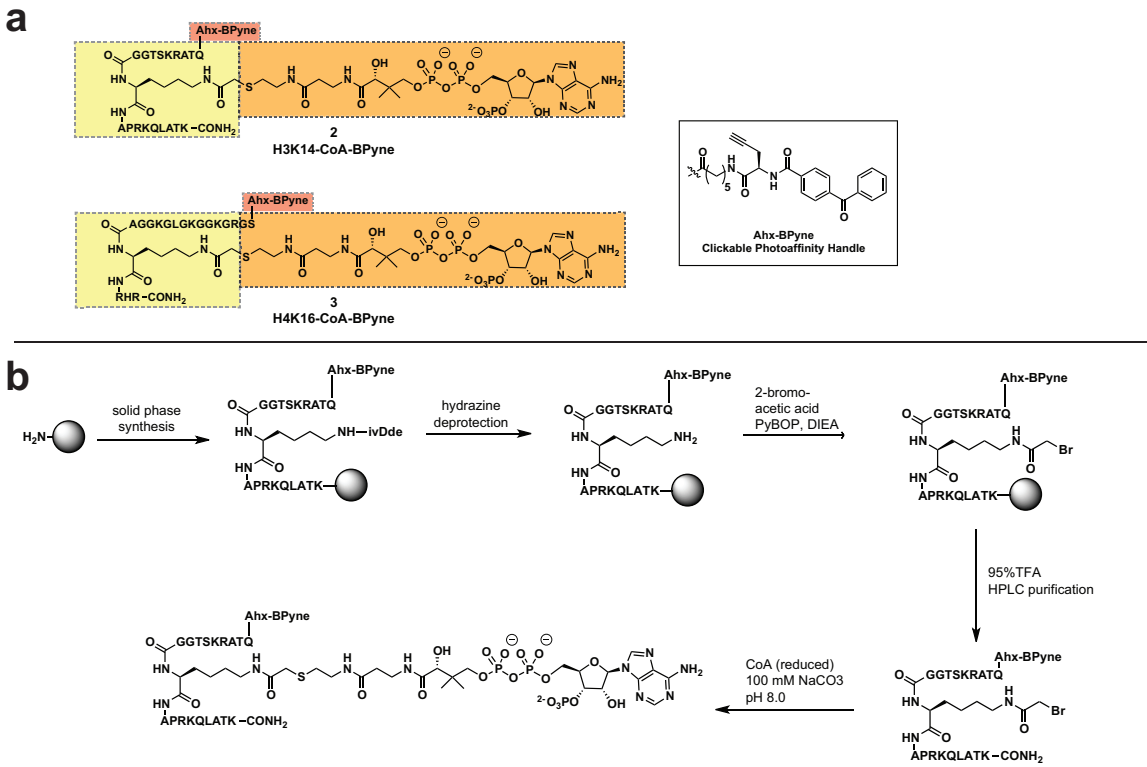


TMR-Biotin-Azide (9)

Figure S15. Structures of TAMRA-azide (8) and TAMRA-biotin azide (9) detection reagents used in this study.



Scheme S1. Scheme for synthesis of Lys-CoA-BPyne probe **1**.



Scheme S2. Scheme for synthesis of H3K14-CoA-BPyne probe **2**. H4K16-CoA-BPyne **3** was synthesized by an analogous route.

Protein	Gene name	H3K14-BPyne (2)	H3K14-BPyne (2)	Control 1	Empty vector 1	Empty vector 2	Average 2-enriched	Average EV	Ratio 2/Control	Ratio 1/EV
Histone acetyltransferase KAT2B	KAT2B	13	18	0	0	0	15.5	0	-	-
Putative beta-actin-like protein 3	POTEKP	7	7	0	3	2	7	2.5	-	2.8
C-1-tetrahydrofolate synthase, cytoplasmic	MTHFD1	4	7	0	3	2	5.5	2.5	-	2.2
Adenylate kinase 2, mitochondrial	AK2	16	4	2	11	5	10	8	5	1.3
Elongation factor 2	EEF2	10	19	3	6	7	14.5	6.5	4.8	2.2
Vimentin	VIM	11	5	2	3	3	8	3	4	2.7
Tubulin beta-2A chain	TUBB2A	10	21	5	5	8	15.5	6.5	3.1	2.4
Stress-70 protein, mitochondrial	HSPA9	20	4	4	13	4	12	8.5	3	1.4
Lactoylglutathione lyase	GLO1	44	46	43	27	35	45	31	1	1.5
78 kDa glucose-regulated protein	HSPA5	27	13	15	18	9	20	14.5	1.3	1.4
Elongation factor 1-alpha 1	EEF1A1	25	19	16	11	10	22	10.5	1.4	2.1

Table S1. Spectral counts for MS/MS analysis of H3K14-CoA-BPyne (2) targets. HEK-293 cell extracts (0.5 mg) were prepared and subjected to H3K14-CoA-BPyne (2) labeling and enrichment as described in the main text. Streptavidin-bound proteins were subjected to on-bead digest and analyzed by LC-MS/MS. Control samples were treated identically except 100 eq of non-covalent competitor H3K14-CoA (5) was added. Abundant proteins (spectral counts >5) showing enrichment ratios of 2-enriched/control > 5 are listed in the main text. Proteins listed in blue represent abundant proteins showing enrichment <5. Proteins listed in green represent proteins non-specifically labeled at high levels by probe 2.

Protein	Gene name	Lys-CoA BPyne (1)	Lys-CoA BPyne (1)	Control 1	Control 2	Average 1- enriched	Average control	Ratio 1/Control	Nucleotide binding
N-alpha-acetyltransferase 50	NAA50	9	10	0	0	9.5	0	-	CoA
Eukaryotic initiation factor 4A-III	EIF4A3	9	10	0	0	9.5	0	-	ATP
26S protease regulatory subunit 8	PSMC5	7	10	0	0	8.5	0	-	ATP
N-acetyltransferase 10	NAT10	9	7	0	0	8	0	-	CoA
Hydroxyacyl-coenzyme A dehydrogenase	HADH	9	9	0	0	9	0	-	CoA
Proteasome subunit beta type-7	PSMB7	7	9	0	0	8	0	-	ATP
26S protease regulatory subunit 6B	PSMC4	5	7	0	0	6	0	-	ATP
Glutamate dehydrogenase 1, mitochondrial	GLUD1	5	7	0	0	6	0	-	NAD(P)
Threonine-tRNA ligase, cytoplasmic	TARS	5	6	0	0	5.5	0	-	ATP
Methylmalonyl-CoA mutase, mitochondrial	MUT	4	8	1	0	6	0.5	12	CoA
ATP-citrate synthase	ACLY	46	83	6	5	64.5	5.5	11.7	ATP, CoA
Isocitrate dehydrogenase	IDH1	14	15	0	3	14.5	1.5	9.7	NAD(P)
Cytosolic acyl coenzyme A thioester hydrolase*	ACOT7	18	18	0	4	18	2	9	CoA
26S protease regulatory subunit 7	PSMC2	46	83	6	5	64.5	5.5	11.7	ATP
Transitional endoplasmic reticulum ATPase	VCP	14	15	0	3	14.5	1.5	9.7	ATP
Acyl-CoA-binding protein	DBI	18	18	0	4	18	2	9	CoA
Inosine-5'-monophosphate dehydrogenase 2	IMPDH2	3	7	1	1	5	1	5	IMP
Succinyl-CoA ligase, beta subunit, mitochondrial	SUCLA2	4	6	0	0	5	0	-	CoA
Histone acetyltransferase P300	EP300	0	0	0	0	0	0	-	CoA

Table S2. Spectral counts for MS/MS analysis of Lys-CoA-BPyne (1) targets. HeLa cell extracts (1 mg) from two separate biological replicates were prepared and subjected to Lys-CoA-BPyne (1) labeling and enrichment as described in the main text. Streptavidin-bound proteins were subjected to on-bead digest and analyzed by LC-MS/MS. Control samples were treated identically except 100 eq of non-covalent competitor Lys-CoA (4) was added. Values in the main text represent average values. The top two proteins exhibiting spectral counts < 5, as well as p300 are shown for posterity

no.	KAT	Uniprot Accession #	References
1	CBP	Q92793	-
2	P300	Q09472	-
3	CLOCK	O15516	-
4	SRC1	Q15788	-
5	SRC3	Q9Y6Q9	-
6	ELP3	Q9H9T3	-
7	HAT1	O14929	-
8	MOZ	Q92794	-
9	MORF	Q8WYB5	-
10	TIP60	Q92993	-
11	MOF	Q9H7Z6	-
12	HBO1	O95251	-
13	TAF1L	Q8IZX4	-
14	TAF1	P21675	-
15	PCAF	Q92831	-
16	GCN5L2	Q92830	-
17	ATAT1	Q5SQI0	-
18	TF3C4	Q9UKN8	-
19	CDY1	Q9Y6F8	³
20	CDY2	Q9Y6F7	³
21	NAA50	Q9GZZ1	⁴
22	NAA60	Q9H7X0	⁵
23	TAU	P10636	⁶
24	ESCO1	Q5FWF5	⁷⁻⁹
25	ESCO2	Q56NI9	⁷⁻⁹
26	NAT10	Q9H0A0	^{10, 11}
27	OGA	O60502	^{12, 13}
28	ATF2	P15336	¹⁴
29	MCMAP	O60318	¹⁵
30	GCN5L1	P78537	¹⁶⁻¹⁹
31	CSRP2BP	Q9H8E8	²⁰
32	ACAT1	P24752	²¹

Table S3. Table of canonical and orphan KATs with Uniprot accession numbers. References are provided for orphan KATs.

General synthetic procedures

Fmoc-amino acids and Rink Amide resin for solid-phase peptide synthesis were purchased from EMD Chemicals. Fmoc-L-propargylglycine was purchased from Anaspec. Coenzyme A, trilithium salt, was obtained from US Biological. Fluorescein-5-isothiocyanate (FITC isomer I) was purchased from Invitrogen. Chromatography solvents were purchased from JT Baker or Macron and used without further purification. Reaction solvents were purchased from Fisher and Aldrich and purified by passage through an aluminum oxide column. Click chemistry detection agents TAMRA-azide **8** and TAMRA-biotin-azide **9** (Figure S15) were synthesized by routes analogous to those previously reported using 5(6)-TAMRA (Anaspec).²² An exemplary procedure is provided for **9**. Analytical HPLC analysis was conducted on an Agilent 1260 Infinity HPLC equipped with a Phenomenex Gemini C18 analytical column (250 x 4.6 mm, 5µm), a diode array detector, and the mobile phase consisting of a gradient of MeCN in 0.1% trifluoroacetic acid (aqueous). HPLC purification was performed using an Agilent 1250 Infinity HPLC equipped with a semi-preparative Phenomenex Gemini C18 column (150 x 21.2 mm, 10 µm). LC-MS analysis was performed on a Shimadzu 2020 LC-MS system. Nominal mass spectra were collected on an Agilent HPLC/MS 1100 series LC/MS system. Matrix-assisted, LASER desorption/ionization time-of-flight mass spectrometry (MALDI-TOF MS) was performed on a Shimadzu Biotech Axima-CFR Plus spectrometer.

Synthesis and characterization data for KAT chemoproteomic probes and parent bisubstrate inhibitors

KAT chemoproteomic probes (**1-3**) and parent bisubstrate inhibitors (**4-6**) were synthesized similarly to previously reported routes by coupling Coenzyme A to the appropriate peptidyl-bromoacetamide precursors (Scheme S1/S2).²³ Exemplary procedures are provided for probes **1-3**, while parent bisubstrate inhibitors **4-6** were synthesized by analogous protocols. N-terminal acetylation for compounds **4-6** was

performed via addition of 4:1:2 DMF:Ac₂O:DIEA. The concentrations of all KAT probes were measured by UV analysis on a Thermo-Fisher Nanodrop 2000 spectrophotometer in distilled and deionized water (ddH₂O) using the molar extinction coefficient (ϵ) for Coenzyme A of 15, 000 M⁻¹cm⁻¹ at λ_{max} of 259 nm.

Lys-CoA-BPyne 1

Lys-CoA-BPyne (**1**) was synthesized on Rink amide resin via manual peptide synthesis. Briefly, a solid-phase peptide synthesis vessel was charged with Rink Amide resin (202 mg, 0.15 mmol), and the resin was swelled in DMF for 30 minutes. The resin was washed with DMF and DCM and deprotected with 20% piperidine in DMF (2 aliquots x 5 min). Deprotection of the resin was monitored by Kaiser test. To the deprotected resin was added a solution of Fmoc-Lys(ivDde)-OH (172 mg, 0.30 mmol), PyBOP (156 mg, 0.30 mmol), and DIEA (209 μ L, 1.2 mmol) in DMF (5 mL). The coupling was allowed to proceed for 2 hours with shaking and monitored by Kaiser test. After coupling, the resin was washed with DMF and DCM and deprotected with 20% piperidine in DMF (2 aliquots x 5 min). This resin was split into two portions (0.075 mmol each) and treated with a solution of with 80 mg Fmoc-Ahx-OH (80 mg, 0.23 mmol), PyBOP (117 mg, 0.23 mmol) and DIEA (105 μ L, 0.60 mmol) in DMF (5 mL). Identical deprotection/coupling procedures were used to install Fmoc-propargylglycine-OH and 4-benzoylbenzoic acid. The ivDde-protected lysine side chain was then deprotected by treatment of the resin with 3% hydrazine in DMF (5 mL) for 2 hours with shaking. To the deprotected resin was added a solution of bromoacetic acid (104 mg, 0.75 mmol) and DIC (117 μ L, 0.75 mmol) in DMF (5 mL). The coupling was allowed to proceed for overnight with shaking and monitored by Kaiser test.

Cleavage from resin was achieved with a 5 mL solution of 95% trifluoroaceticacid (TFA), 2.5% triisopropylsilane, and 2.5% water, and shaking for 1.5 hours. Next, the cleavage solution was filtered and the resin washed with an additional 1 mL TFA. Excess TFA was removed with a gentle stream of air to reduce the volume to 1-2 mL, and the compound was precipitated with chilled diethyl ether and pelleted via centrifugation. The pellet was dissolved in water with 0.1% TFA and split into 5 portions, one of which was directly purified via reverse phase preparative HPLC. After lyophilization of the purified peptide, it was dissolved in 100 mM pH 8 NaHCO₃ (1 mL), and to this solution was added Coenzyme A tritium salt (10mg, 0.013 mmol). The solution was stirred for 30 minutes, diluted with aqueous 0.1% TFA (5 mL), and 1 M HCl was added dropwise to adjust the solution to pH 2. This solution was again directly purified via preparative HPLC, and lyophilized to provide 4.9 mg (3.6 µmol) of compound **1** (24% overall yield).

H3K14-CoA-BPyne 2

Automated peptide synthesis of an H3K14 peptide with the sequence QTARKSTGGK(ivDde)APRKQLATK was carried out using an Applied Biosystems 433A Peptide Synthesizer (ABI) using 0.368 mg Rink Amide resin (0.68 mmol/g), using Fmoc-based solid-phase peptide chemistry with HCTU activation. After final Fmoc deprotection of the N-terminus, sequential coupling/deprotection steps were performed manually to install Fmoc-Ahx-OH, Fmoc-propargylglycine-OH, and 4-benzoylbenzoic acid using similar conditions as for compound **1** on 0.05 mmol resin. Cleavage from resin, coupling to Coenzyme A, and purification were similarly performed to yield 27 mg (8.3 µmol) of compound **2** (16% overall yield).

H4K16-CoA-BPyne 3

Automated solid-phase synthesis of an H4 peptide with the sequence SGRGKGGKGLGKGGAK(ivDde)RHR was carried out in a similar manner as for the H3K14 peptide described above. Analogous functionalization and purification steps provided 3.7 mg (1.2 µmol) of compound **3** (2.4% overall yield).

Scale and yields for synthesis of photoaffinity probes and parent bisubstrates

Lys-CoA-BPyne (**1**): Theoretical yield: 15 µmol. Actual yield: 3.6 µmol (24%).

H3K14-CoA-BPyne (**2**): Theoretical yield: 50 µmol. Actual yield: 8.3 µmol (17%).

H4K16-CoA-BPyne (**3**): Theoretical yield: 50 µmol. Actual yield: 1.2 µmol (2.4%).

Lys-CoA (**4**): Theoretical yield: 118 µmol. Actual yield: 32 µmol (27%).

H3K14-CoA (**5**): Theoretical yield: 25 µmol. Actual yield: 3.7 µmol (15%).

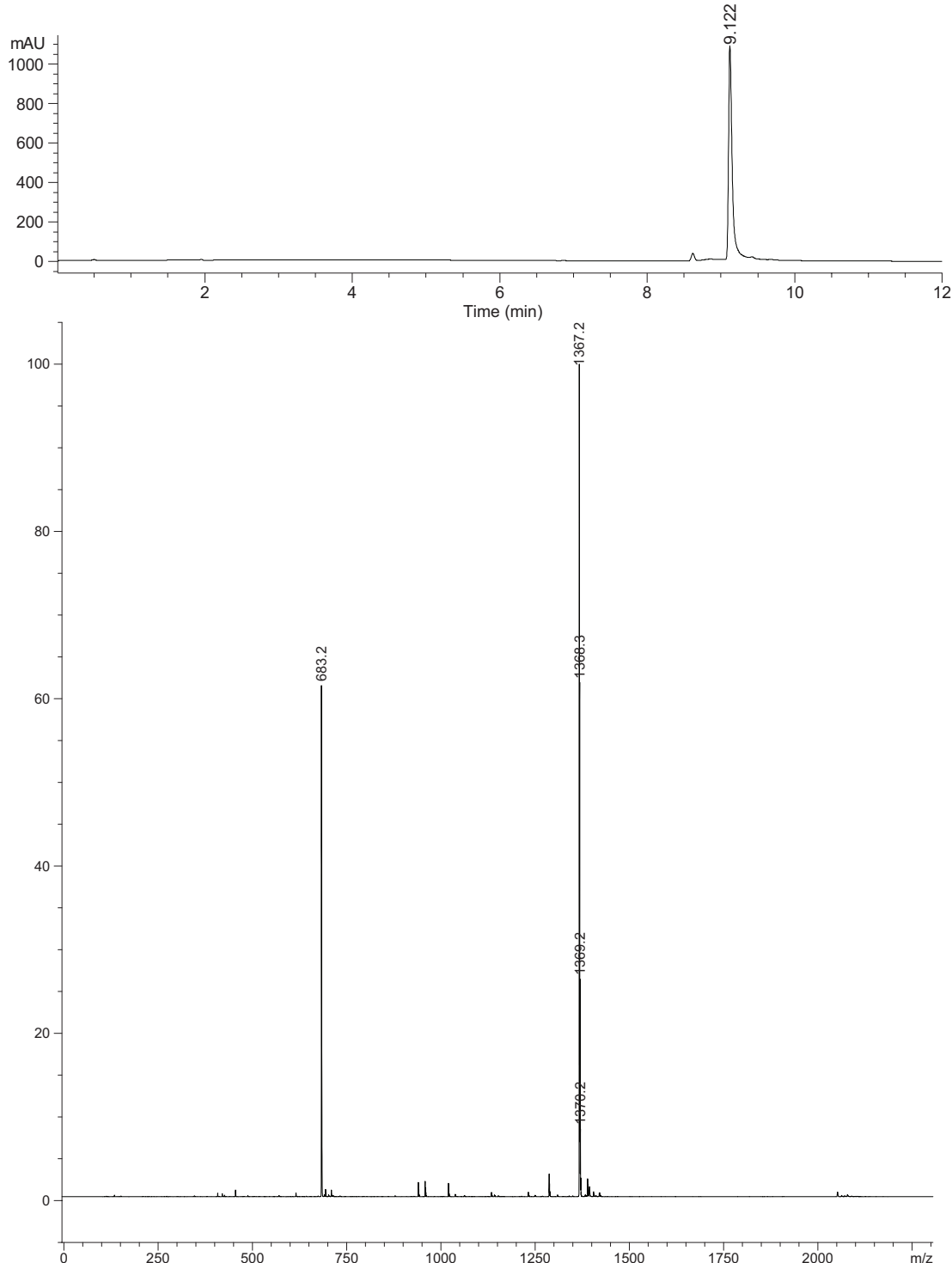
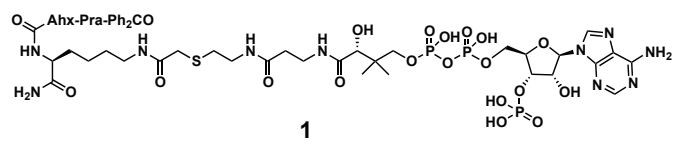
H4K16-CoA (**6**): Theoretical yield: 56 µmol. Actual yield: 2.4 µmol (3.9%).

TMR-biotin-azide (Trifunctional Click Reagent) **9**

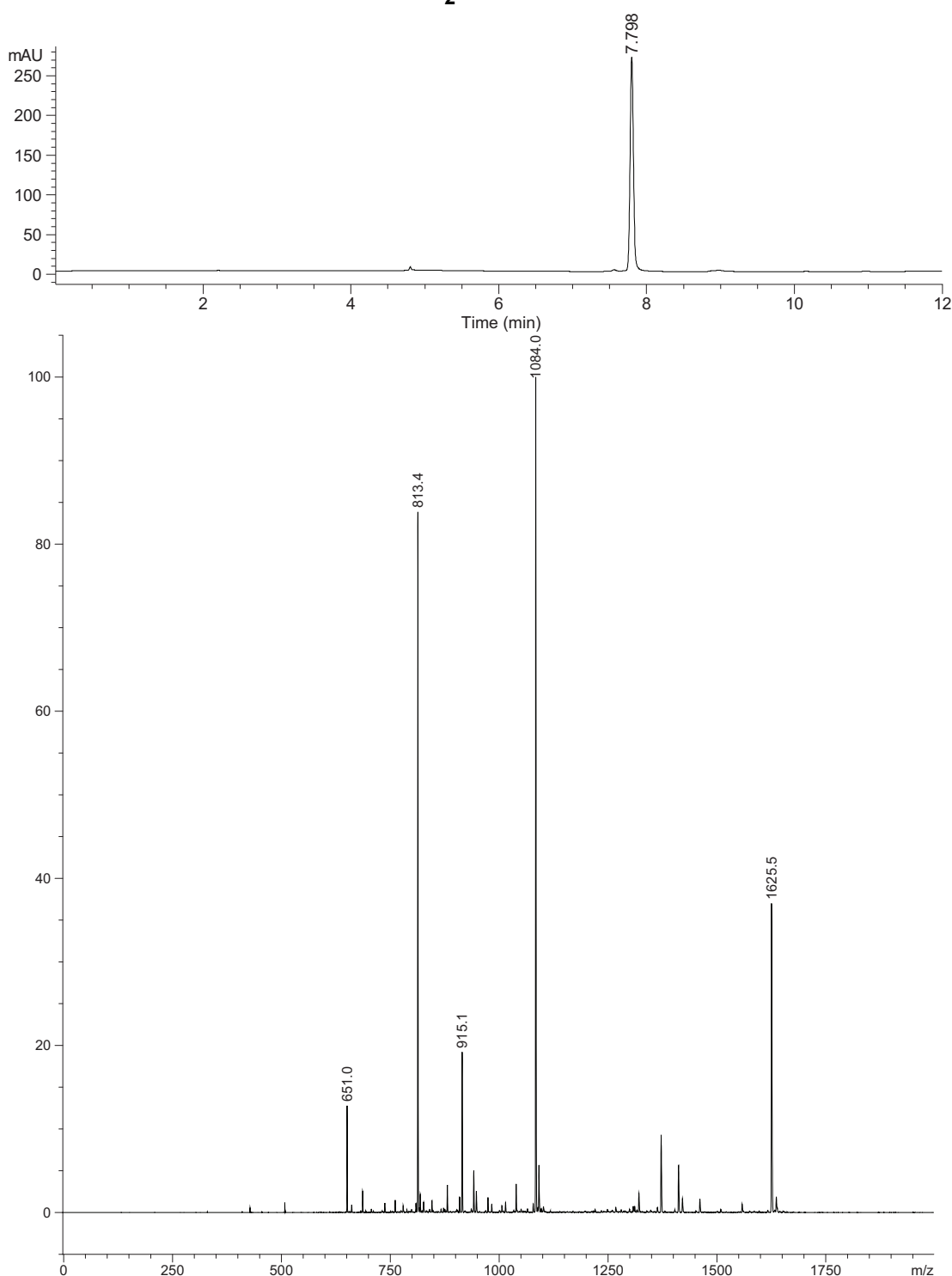
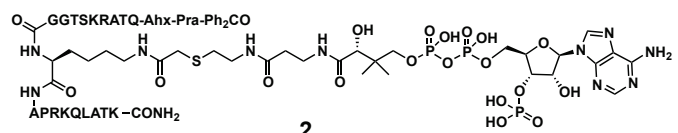
A solid-phase peptide synthesis vessel was charged with Rink Amide resin (47 mg, 0.035 mmol), and the resin was swelled in DMF for 30 minutes. The resin was washed with DMF and DCM and deprotected with 20% piperidine in DMF (2 aliquots x 5 min). Deprotection of the resin was monitored by Kaiser test. To the deprotected resin was added a solution of Fmoc-Lys(Boc)-OH (66 mg, 0.14 mmol), PyBOP (73 mg, 0.14 mmol), and DIEA (49 µL, 0.28 mmol) in DMF (5 mL). Identical deprotection/coupling procedures were used to install Fmoc-Lys(N₃)-OH and Fmoc-Ahx-OH. Next, 5(6)-TAMRA (45 mg, 0.105 mmol), diisopropylcarbodiimide (16.4 µL, 0.105 mmol), and Oxyma Pure (14.9 mg, 0.105 mmol) were added in 5 mL DMF and the coupling proceeded overnight with shaking. Cleavage from resin was achieved with a 5

mL solution of 95% trifluoroaceticacid (TFA), 2.5% triisopropylsilane, and 2.5% water, and shaking for 1.5 hours. Next, the cleavage solution was filtered and the resin washed with an additional 1 mL TFA. Excess TFA was removed with a gentle stream of air to reduce the volume to 1-2 mL, and the compound was precipitated with chilled diethyl ether and pelleted with centrifugation. The pellet was dissolved in aqueous 0.1% TFA and directly purified via reverse phase preparative HPLC. Both isomers were collected, combined and lyophilized.

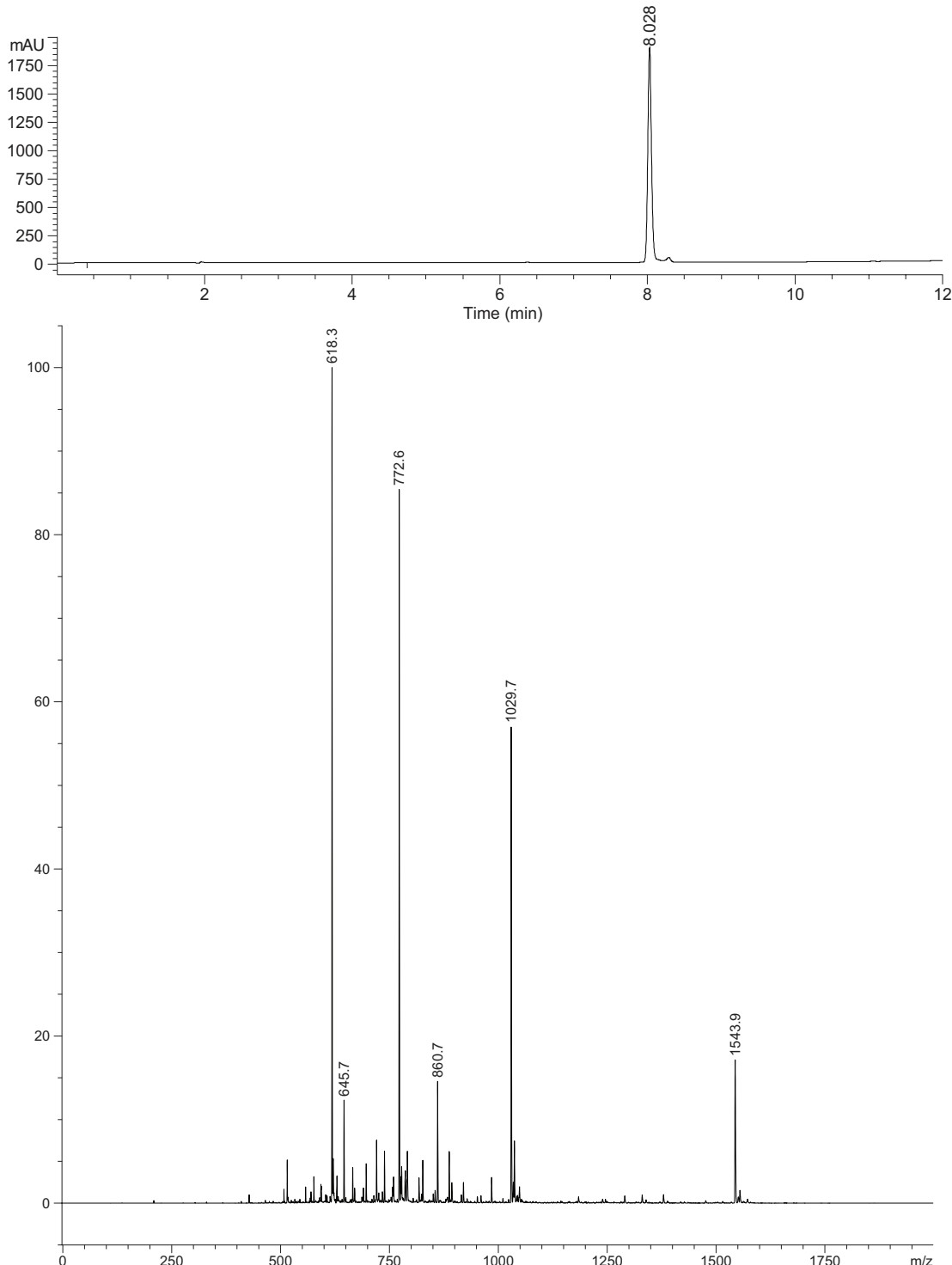
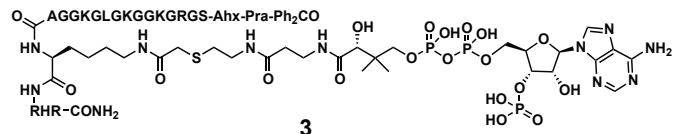
The dark purple lyophilized powder was next dissolved in 2 mL DMSO, and to this solution was added EZ-link NHS-PEG₄ Biotin (41 mg, 0.035 mmol) and DIEA (49 µL, 0.28 mmol), and this mixture was stirred for 30 minutes, then diluted with 5 mL aqueous 0.1% TFA and purified by preparative HPLC. Lyophilization provided 18 mg (14 µmol) of compound **9** (40% yield).



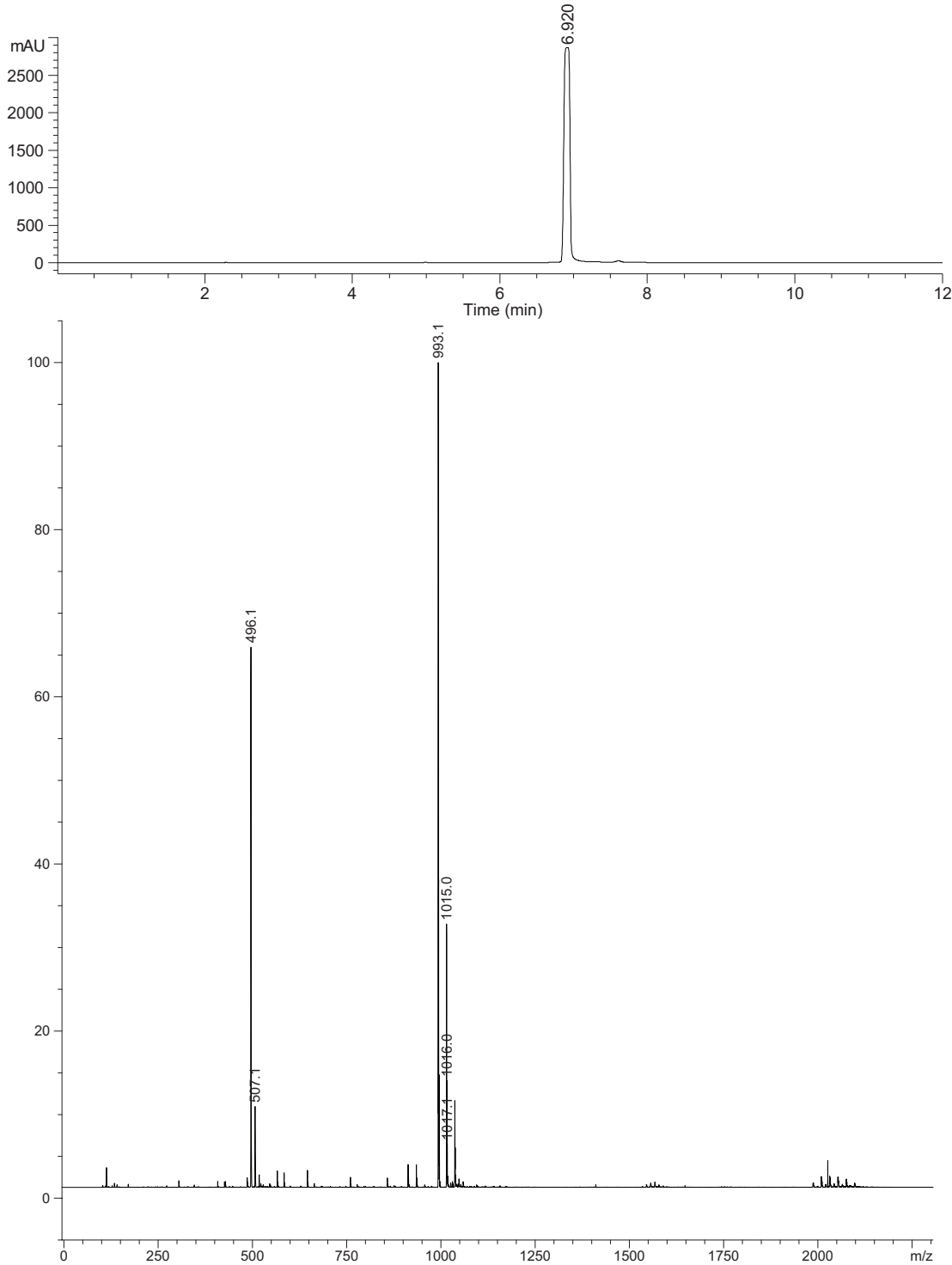
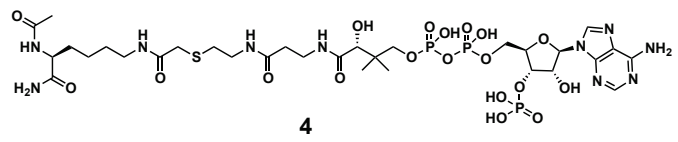
Lys-CoA-BPyne (1): HPLC (top) and ESI (negative mode) data for compound **1**. $[M-H]^-$ calc'd for $C_{54}H_{74}N_{12}O_{22}P_3S^-$: 1367.4, $[M-2H]^{2-}$: 683.2.



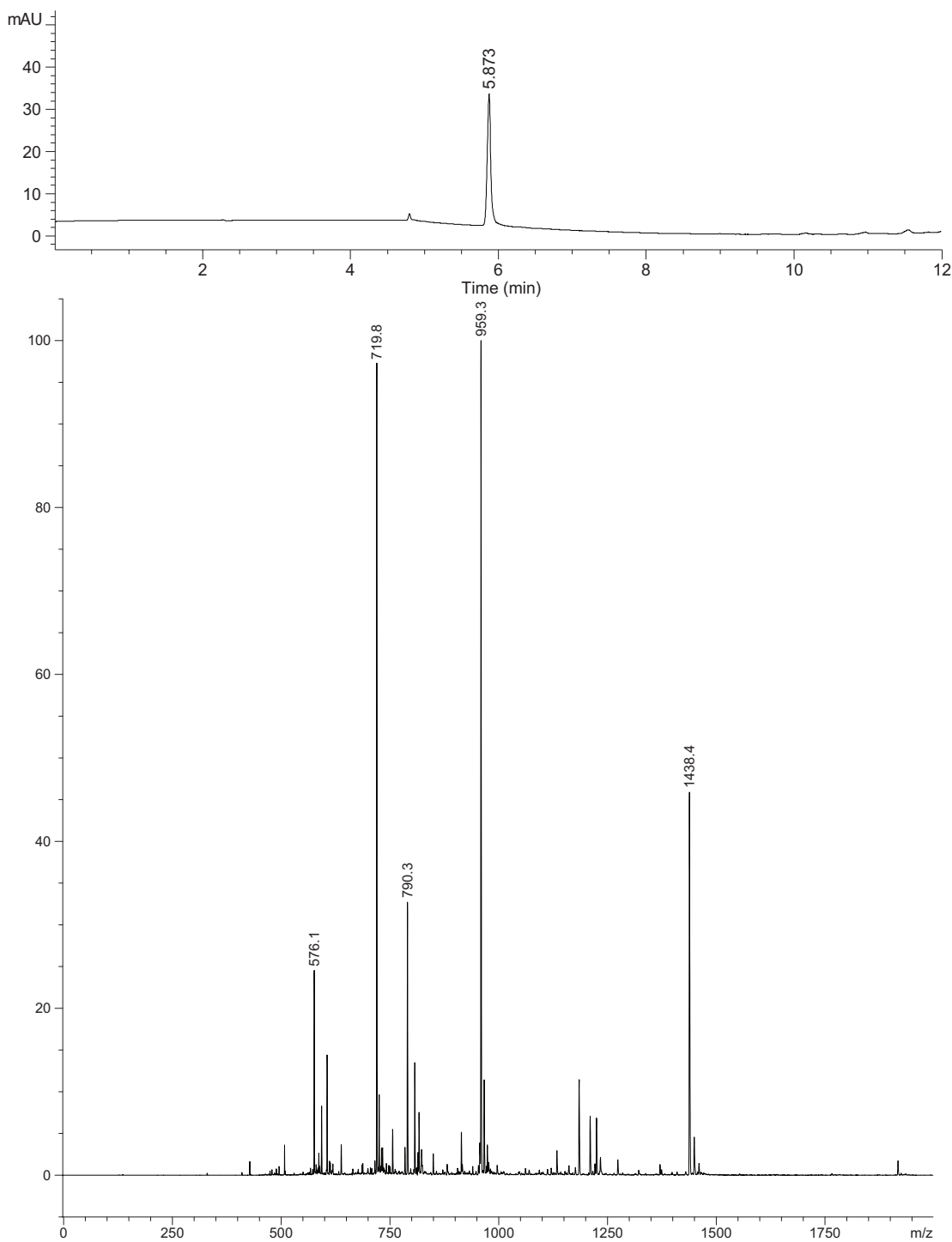
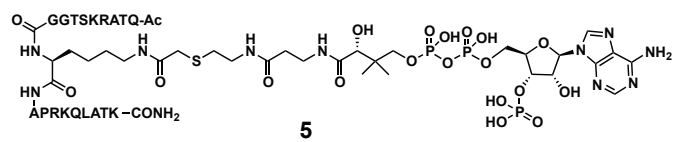
H3K14-CoA-BPyne (2): HPLC (top) and ESI data for compound **2**. $[M+H]^+$ calc'd for $C_{133}H_{217}N_{41}O_{46}P_3S^+$: 3249.5, $[M+2H]^{2+}$: 1625.7, $[M+3H]^{3+}$: 1084.2, $[M+4H]^{4+}$: 813.4, $[M+5H]^{5+}$: 650.9.



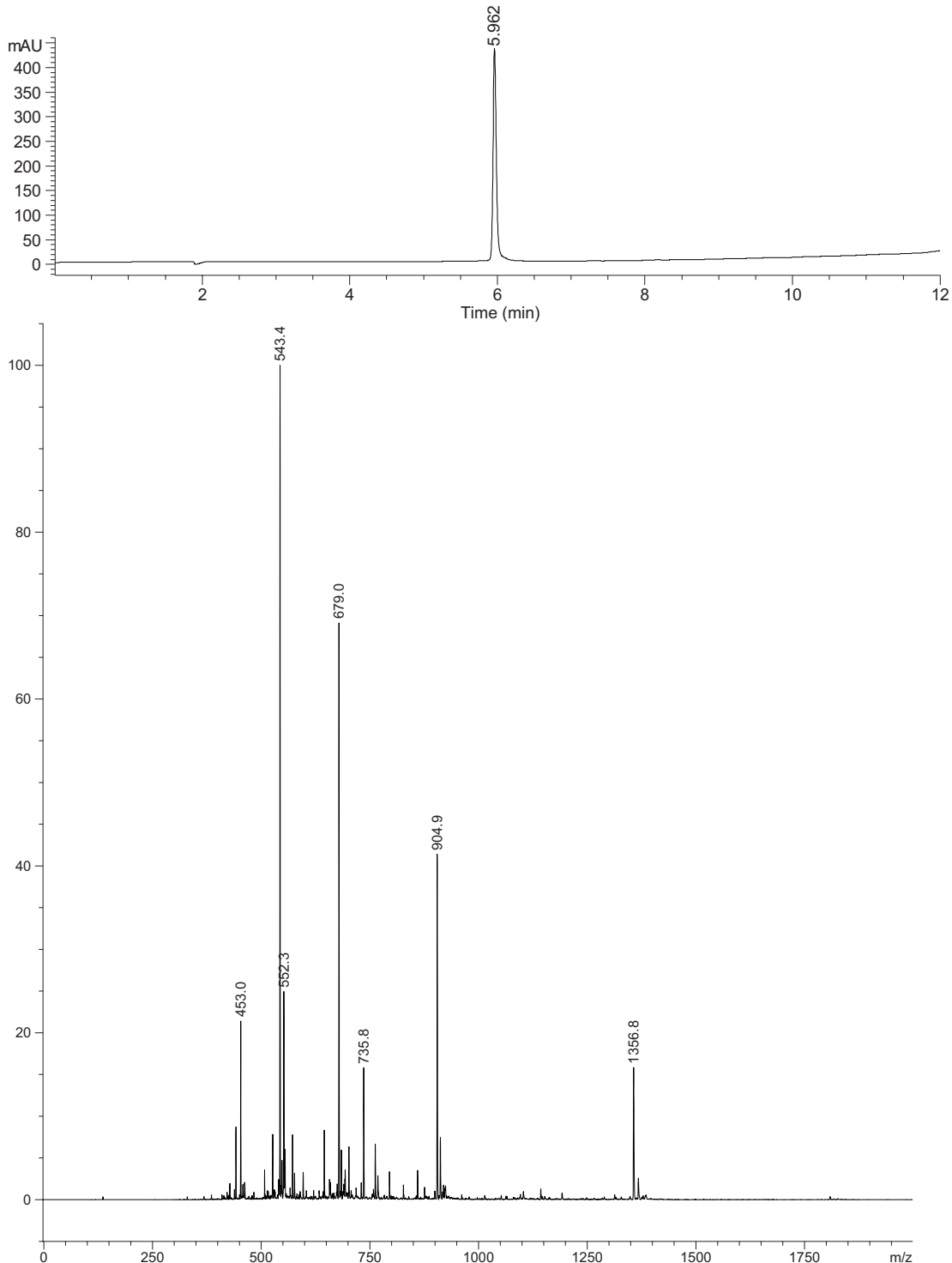
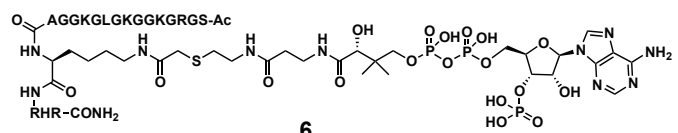
H4K16-CoA-BPyne (3): HPLC (top) and ESI data for compound **3**. $[M+H]^+$ calc'd for $C_{124}H_{200}N_{44}O_{41}P_3S^+$: 3086.4, $[M+2H]^{2+}$: 1543.7, $[M+3H]^{3+}$: 1029.5, $[M+4H]^{4+}$: 772.3, $[M+5H]^{5+}$: 618.1.



Lys-CoA (4): HPLC (top) and ESI (negative mode) data for compound **4**. $[M-H]^-$ calc'd for $C_{31}H_{52}N_{10}O_{19}P_3S^-$: 993.2, $[M-2H+Na]^-$: 1015.2, $[M-2H]^{2-}$: 496.1.



H3K14-CoA (5): HPLC (top) and ESI data for compound 5. $[M+H]^+$ calc'd for $C_{110}H_{195}N_{39}O_{43}P_3S^+$: 2875.3, $[M+2H]^{2+}$: 1438.2, $[M+3H]^{3+}$: 959.1, $[M+4H]^{4+}$: 719.6, $[M+5H]^{5+}$: 575.9.



H3K14-CoA (6): HPLC (top) and ESI data for compound **6**. $[M+H]^+$ calc'd for $C_{101}H_{178}N_{42}O_{38}P_3S^+$: 2712.2, $[M+2H]^{2+}$: 1356.6, $[M+3H]^{3+}$: 904.7, $[M+4H]^{4+}$: 678.8, $[M+5H]^{5+}$: 543.2, $[M+6H]^{6+}$: 452.9.

References:

1. Arrowsmith, C. H., Bountra, C., Fish, P. V., Lee, K., and Schapira, M. (2012), *Nat Rev Drug Discov* 11, 384-400.
2. Liu, L., Zhen, X. T., Denton, E., Marsden, B. D., and Schapira, M. (2012), *Bioinformatics* 28, 2205-2206.
3. Lahn, B. T., Tang, Z. L., Zhou, J., Barndt, R. J., Parvinen, M., Allis, C. D., and Page, D. C. (2002), *Proc Natl Acad Sci U S A* 99, 8707-8712.
4. Evjenth, R., Hole, K., Karlsen, O. A., Ziegler, M., Arnesen, T., and Lillehaug, J. R. (2009), *J Biol Chem* 284, 31122-31129.
5. Yang, X., Yu, W., Shi, L., Sun, L., Liang, J., Yi, X., Li, Q., Zhang, Y., Yang, F., Han, X., Zhang, D., Yang, J., Yao, Z., and Shang, Y. (2011), *Mol Cell* 44, 39-50.
6. Cohen, T. J., Friedmann, D., Hwang, A. W., Marmorstein, R., and Lee, V. M. (2013), *Nat Struct Mol Biol* 20, 756-762.
7. Bellows, A. M., Kenna, M. A., Cassimeris, L., and Skibbens, R. V. (2003), *Nucleic Acids Res* 31, 6334-6343.
8. Hou, F., and Zou, H. (2005), *Mol Biol Cell* 16, 3908-3918.
9. Zhang, J., Shi, X., Li, Y., Kim, B. J., Jia, J., Huang, Z., Yang, T., Fu, X., Jung, S. Y., Wang, Y., Zhang, P., Kim, S. T., Pan, X., and Qin, J. (2008), *Mol Cell* 31, 143-151.
10. Chi, Y. H., Haller, K., Peloponese, J. M., Jr., and Jeang, K. T. (2007), *J Biol Chem* 282, 27447-27458.
11. Shen, Q., Zheng, X., McNutt, M. A., Guang, L., Sun, Y., Wang, J., Gong, Y., Hou, L., and Zhang, B. (2009), *Exp Cell Res* 315, 1653-1667.
12. Toleman, C., Paterson, A. J., Whisenhunt, T. R., and Kudlow, J. E. (2004), *J Biol Chem* 279, 53665-53673.
13. Butkinaree, C., Cheung, W. D., Park, S., Park, K., Barber, M., and Hart, G. W. (2008), *J Biol Chem* 283, 23557-23566.
14. Kawasaki, H., Schiltz, L., Chiu, R., Itakura, K., Taira, K., Nakatani, Y., and Yokoyama, K. K. (2000), *Nature* 405, 195-200.
15. Takei, Y., Swietlik, M., Tanoue, A., Tsujimoto, G., Kouzarides, T., and Laskey, R. (2001), *EMBO Rep* 2, 119-123.
16. Webster, B. R., Scott, I., Traba, J., Han, K., and Sack, M. N. (2014), *Biochim Biophys Acta*.
17. Scott, I., Webster, B. R., Chan, C. K., Okonkwo, J. U., Han, K., and Sack, M. N. (2014), *J Biol Chem* 289, 2864-2872.
18. Webster, B. R., Scott, I., Han, K., Li, J. H., Lu, Z., Stevens, M. V., Malide, D., Chen, Y., Samsel, L., Connelly, P. S., Daniels, M. P., McCoy, J. P., Jr., Combs, C. A., Gucek, M., and Sack, M. N. (2013), *J Cell Sci* 126, 4843-4849.
19. Scott, I., Webster, B. R., Li, J. H., and Sack, M. N. (2012), *Biochem J* 443, 655-661.
20. Guelman, S., Kozuka, K., Mao, Y., Pham, V., Solloway, M. J., Wang, J., Wu, J., Lill, J. R., and Zha, J. (2009), *Mol Cell Biol* 29, 1176-1188.
21. Fan, J., Shan, C., Kang, H. B., Elf, S., Xie, J., Tucker, M., Gu, T. L., Aguiar, M., Lonning, S., Chen, H., Mohammadi, M., Britton, L. M., Garcia, B. A., Aleckovic, M., Kang, Y., Kaluz, S., Devi, N., Van Meir, E. G., Hitosugi, T., Seo, J. H., Lonial, S.,

- Gaddh, M., Arellano, M., Khoury, H. J., Khuri, F. R., Boggon, T. J., Kang, S., and Chen, J. (2014), *Mol Cell* 53, 534-548.
22. Speers, A. E., and Cravatt, B. F. (2004), *Chem Biol* 11, 535-546.
23. Zheng, Y., Thompson, P. R., Cebrat, M., Wang, L., Devlin, M. K., Alani, R. M., and Cole, P. A. (2004), *Methods Enzymol* 376, 188-199.